

Optimization of Biomimetic Hair Sensors

N. Izadi, R. K. Jaganatharaja, and G. J. M. Krijnen, *Member, IEEE*

Abstract— High density arrays of artificial hair sensors, biomimicking the extremely sensitive mechanoreceptive filiform hairs found on cerci of crickets have been fabricated. We assess the sensitivity of these artificial sensors and present a scheme for further optimization addressing the deteriorating effects of stress in the structures. We show that, by removing a portion of Chromium electrodes close to the torsional beams, the upward deflection at the edges of the membrane due to the stress, will decrease hence increase the sensitivity.

Index Terms—Biomimetic, Flow Sensor, Sensitivity, Optimization, Pull-in Voltage

I. INTRODUCTION

FILIFORM hair based mechanoreceptors on the abdominal appendages (cerci) of crickets are extremely sensitive flow sensors for particle displacement detection with sensitivities bordering thermal noise threshold [1] (Figure (1)). The large number of hairs as well as their directivity results in a system capable of complex flow pattern detection, hence recognition of nearby movements with high directional resolution [2]. They make crickets capable of effectively detecting an approaching predator and reacting accordingly. Flow sensors based on drag force induced rotation are interesting engineering objects since they allow for high-density arrays which are impractical or impossible with the more common hot wire anemometers (HWA) or microflow [3].

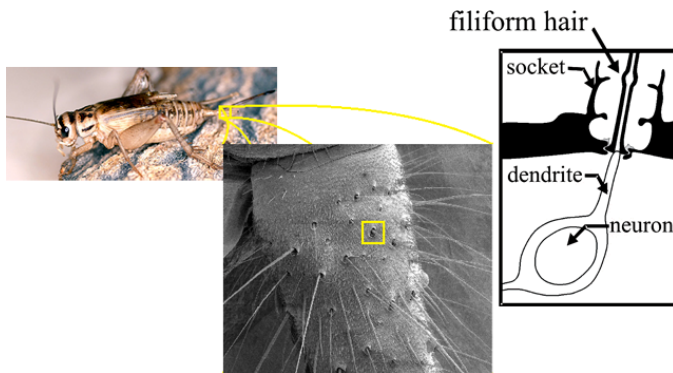


Figure 1. Filiform hairs on the cerci of crickets (Courtesy of J. Casas and coworkers, IRBI, Univ. de Tours)

Manuscript received October 1, 2007. The Customized Intelligent Life-Inspired Arrays project is funded by the Future and Emergent Technologies arm of the IST Program.

Authors are with the Transducer Science and Technology group, MESA⁺ and IMPACT Research Institutes, University of Twente, Postbus 217, 7500 AE Enschede The Netherlands (phone: 053-489-4438; fax: 053-489-3343; email: n.izadi@ewi.utwente.nl).

In recent years mimicking nature to realize more sensitive, robust and reliable sensors has become an appealing practice in micromachining technology. Biomimetic hair structures [4-6] promise low cost, small, sensitive and fast response flow sensors to use in robotic, vehicle control and pathfinder applications, to mention a few.

In previous work we have shown artificial SU-8 hair sensors based on capacitive readout of flow-induced tilting of a silicon nitride membrane with Chromium electrodes deposited on top [7]. Figure (2) shows a schematic of these sensors. Fluid flow exerts a drag force on protruding hairs. The resulting drag torque induces a tilting of the hairs from their normal upright position which results in membrane deflection and capacitance changes accordingly.

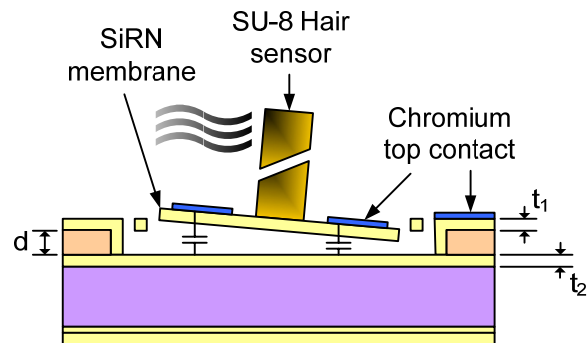


Figure 2. Artificial hair schematic

Figure (4) shows an SEM micrograph of (the base of) a fabricated sensor. It can be clearly seen that the membranes are curved. This leads to reduced performance.

In this paper we first introduce our capacitive hair sensors' operation principle and determine their sensitivity and electrostatic spring softening coefficient. Then we consider the effect of membrane curvature on the sensitivity and investigate the effects which result in the curvature. To reduce the detrimental effects of curvature we propose a new design for the electrodes and explain the according increase in sensitivity. We also discuss the effect of DC bias on sensitivity and adaptability of the sensor.

II. SENSOR MODEL

A. Mechanical model and Adaptability

The mechanoreceptive cercal hair of the crickets has been thoroughly analyzed and its operational mechanics is very often compared to that of an inverted pendulum model [2]. The hair as an inverted pendulum, a typical second-order

mechanical system, is described by its mechanical parameters: (i) moment of Inertia J , (ii) spring constant S_0 , and (iii) torsional resistance R (see figure (3)).

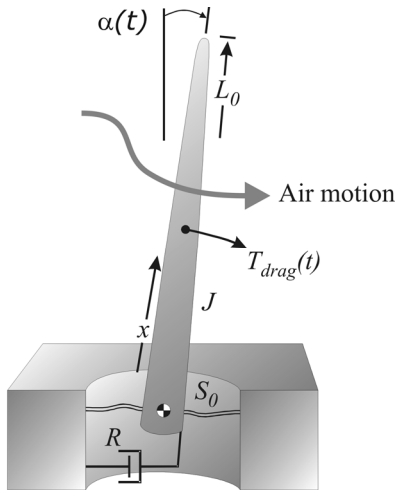


Figure 3. Hairs can be modeled as an inverted pendulum which represents a second order mechanical system [1]

As explained before, the recently presented artificial hair sensors are based on the capacitive read-out of flow-induced tilting (α) of an SU-8 hair mounted on a Silicon Nitride membrane. Thin Chromium electrodes, deposited on top of the Silicon Nitride membrane and the conductive Silicon substrate form the top and bottom electrodes of the sensing capacitor, respectively.

The sensitivity of the device can be derived [8] as follow:

$$\frac{\partial C}{\partial \alpha} = \lim_{\alpha \rightarrow 0} \frac{\partial}{\partial \alpha} \left(\int_A \frac{\epsilon_0 dA}{d' + x \sin \alpha} \right) = \frac{\epsilon_0 W L^2}{d'^2} \quad (1)$$

in which

$$d' = d + \frac{t_1 + t_2}{\epsilon_r} \quad (2)$$

is the dielectric thickness and where R is the radius of the membrane. In this case R is $85 \mu\text{m}$, the gap between the electrodes (d) is typically $1 \mu\text{m}$, the thickness of the silicon nitride layers t_1 and t_2 are $1 \mu\text{m}$ and $0.1 \mu\text{m}$ respectively, ϵ_0 and ϵ_r are dielectric constant of air and the relative dielectric constant of silicon nitride, respectively.

Additionally, we have shown [8] that by making use of the electrostatic spring softening effect based on the theory of transduction, the torsional stiffness can be varied on application of a DC bias voltage (U) across the electrodes. Then the effective torsional spring stiffness (S_{eff}) is given as:

$$S_{eff} = S_0 - U^2 \kappa = S_0 (1 - U^2 \frac{\kappa}{S_0}) \quad (3)$$

where, S_0 is the torsional stiffness of the springs, without any applied bias voltage and κ is the coefficient of effective spring softening given by

$$\begin{aligned} \kappa &= \frac{1}{2} \frac{\partial^2 C}{\partial \alpha^2} = \frac{1}{2} \lim_{\alpha \rightarrow 0} \frac{\partial^2}{\partial \alpha^2} \left(\int_A \frac{\epsilon_0 dA}{d' + x \sin \alpha} \right) \\ &= \frac{\epsilon_0 W L^3}{3 d'^3} \end{aligned} \quad (4)$$

By applying DC-bias voltages, the sensor can be adaptively tuned for higher sensitivities. Moreover, by altering the effective torsional stiffness of the springs, the resonance frequency of the structure will be modified, allowing the sensor to adapt to a desired working range.

High sensitivity and adaptability of the sensors, which are highly sought, depend mainly on the shape of the sensor capacitance, which in turn relies strongly on the quality of the fabricated membrane and the electrode design. Slight degradation in the quality, for instance, curvature in the Silicon Nitride membrane, can affect the sensitivity and coefficient of effective spring softening in a deteriorating way.

B. Curvature effect

Fabrication of the presented hair sensors is discussed in detail in [7]. Large arrays of hair sensors with two primary electrode designs on circular and rectangular membranes were fabricated.

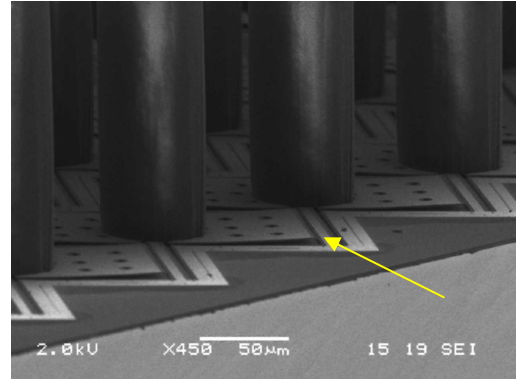


Figure 4. SEM image of rectangular membranes. The membranes are curved upward at the edge

Figure (4) shows a SEM image of rectangular membranes, with a slight curvature. This curvature of the membrane is primarily due to the tensile stress present in the Chromium thin layer, deposited on top of the Nitride membrane. The curvature results in an undesired increase in the gap between the electrodes, leading to a significant decrease in the sensitivity.

The curvature can be approximated by a part of a circle with a radius of curvature, R_c , which is determined from the measurements. Considering the effect of this bending as $\delta(x)$, which can be obtained according to Stoney's formula, we can write the sensitivity as

$$\int_A \frac{\epsilon_0 W x dx}{(d' + x \sin \alpha + \delta(x))^2} \quad (5)$$

Numerical evaluation of equation (5) shows a great reduction in sensitivity in comparison with equation (1).

C. Curvature Optimization

As we showed in the previous section membrane curvature has a great detrimental effect on capacitance, sensitivity and electrostatic spring softening (ESS) coefficient. For example, the sensitivity of a circular membrane falls off 4 times and the ESS coefficient decreases by 9.5 times due to membrane curvature of $2.5 \mu\text{m}$ [8]. Therefore, it is preferable to reduce this curvature. The Silicon Nitride layer is deposited by an optimized low-stress LPCVD process and hence, the tensile stress is negligible [8]. Therefore it can be considered as a flat substrate. The bending moment due to tensile stress in the Chromium layer increases with the thickness. Reducing the electrode thickness is one way to reduce curvature but this has been minimized in the current sensors to 50 nm and there are serious issues regarding electrode resistance on further reduction.

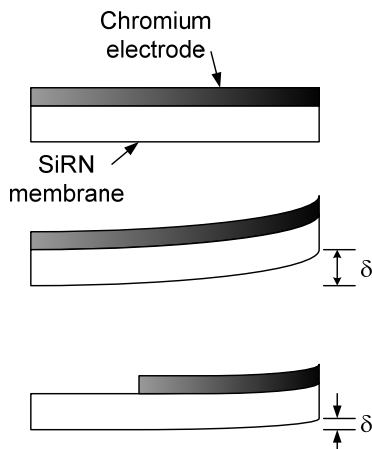


Figure 5. Decreasing the electrode length will reduce the upward deflection at the edge of membrane

The electrode area near the torsional beams has minor effect on the sensor's sensitivity since there is little change in the height of this area on membrane tilt. Therefore, whereas this area plays a major role in the total capacitance, it hardly contributes to the change of capacitance on tilt. On the other hand, by reducing the electrode area as shown in figure (5), the maximum upward deflection at the edge of the membrane decreases thereby increasing the sensitivity. Hence it is logical to remove a portion of the electrode close to the torsional beams.

It has been shown [8] that this will result in considerable increase of sensitivity and ESS coefficient.

Figure (6) shows the actual sensitivity and electrostatic spring softening (ESS) coefficient as a function of the length of the electrode-less area for a rectangular membrane. The calculation is based on $3 \mu\text{m}$ deflection at the edge of membrane which had been obtained using White Light Interferometer [8].

As it can be seen in the figure, decreasing the electrode length increases the sensitivity initially due to reduction in curvature and reaches a maximum. Further reduction will decrease the sensitivity as the reduction in the total

capacitance becomes a dominant factor. Like the sensitivity, larger kappa is achieved by reducing the area to some extent but again this is not a monotonic increasing function. The electrode-less area can be optimized to have sensors with maximum sensitivity and electrostatic spring softening coefficient.

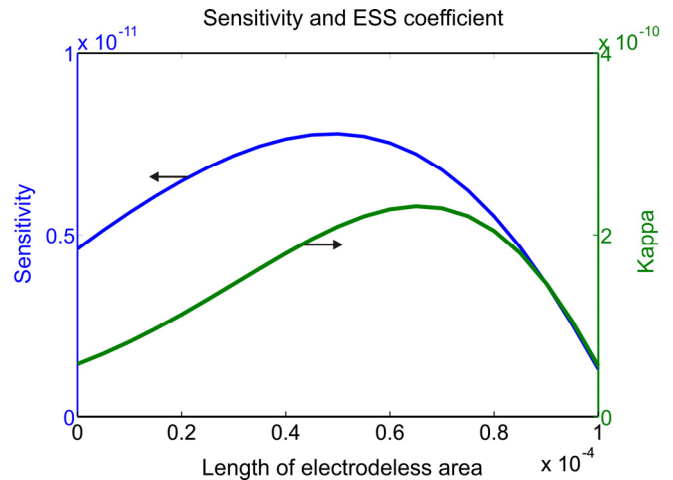


Figure 6. Rectangular membrane sensitivity and ESS changes with respect to length of electrode-less area

D. DC Bias effect

As we apply a DC bias to adapt the sensor to a desirable working range the resultant electric field between the electrodes will have several effects on the sensor parameters. Firstly electrodes attract each other so the gap between them will decrease.

Secondly, applying DC bias will produce a force on the electrodes which in turn results in a bending moment on the membrane and reduces the curvature [9]. This curvature reduction can be calculated by equating electrostatic force and mechanical restoring force at the point of equilibrium.

E. Sensitivity of optimized biased sensor

As we saw decreasing the electrode area in a proper way will increase the sensitivity. If a specific DC bias is chosen according to situation criteria, because the membrane curvature will be reduced by application the bias, we need to reconsider the sensitivity behavior as a function of electrode area. Figure (7) shows the change in device sensitivity as a function of electrodeless area for five different DC biases below vertical pull-in voltage. It can be seen that the higher the bias, the lesser is the effect of reducing the electrode area. This is obviously because the effect of the electric field results from DC bias decreases as the electrode area become smaller.

The sudden reduction in the beginning of the purple curve is due to the fact that near pull-in voltage the membrane deflects downward so the gap between electrodes is less at the edge of the membrane than the intended gap. Reducing the electrode length will cause a decrease in the electric field and hence the moment that bends the membrane. Therefore the membrane becomes more flat hence sensitivity decreases. It is also conclusive that if we decrease the electrode length more

than half there will be no effect of DC biasing on sensitivity. It also holds to some extent for the maximum point. Especially as we see in the next part the pull-in voltage caused by rotational instability decreases as the ESS coefficient increases. It means that there is a tradeoff between the increase in sensitivity by reducing the electrode length and available room for adaptability.

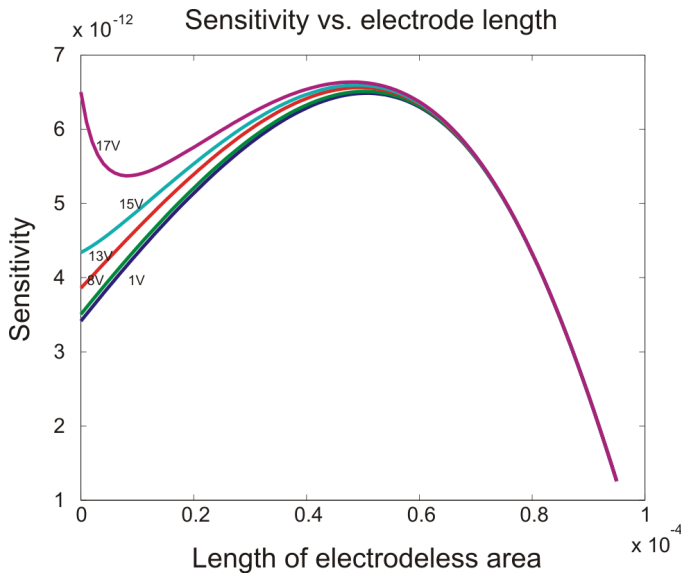


Figure 7. Change in sensitivity according to electrodeless area at different DC biases

F. Pull-in Voltage

Figure (8) shows the vertical pull-in voltage as a function of the length of electrodeless area.

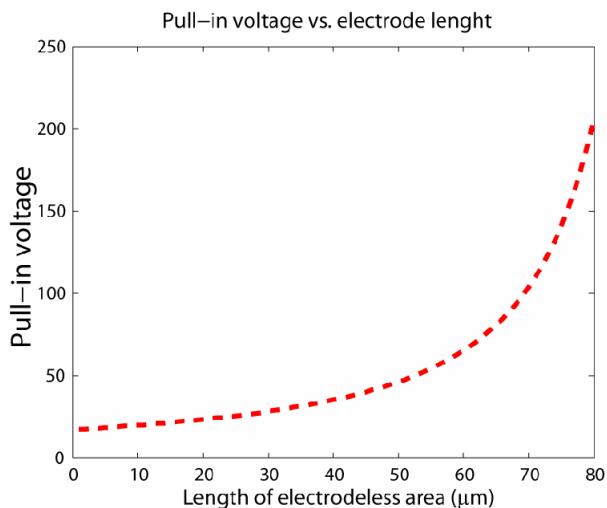


Figure 8. Vertical pull-in voltage versus length of electrodeless area

It is obvious that as the electrode area decreases the electrostatic force decreases. Therefore the force that is needed to pull in the membrane will be reached at higher voltages. In figure (8) we plot the voltage at the onset of pull-in versus electrodeless area length for a rectangular membrane. It also can be derive analytically [9] for a flat

membrane by first order approximation as

$$V_{pull-in} = \sqrt{\frac{8}{27} \cdot \frac{K_r d'}{\epsilon_0 W L}} \quad (6)$$

Note that in equation (6) L is the length of the electrode which decreases along the abscissa in figure (8). In addition equation (6) gives a lower limit for the pull-in voltage since the actual gap between electrodes is bigger due to upward curvature.

Although the vertical pull-in voltage increases monotonically when decreasing the electrode length the rotational instability which results from diminishing effective spring constant (see equation (3)) governs the pull-in voltage. Rotational instability can be found [10] as

$$V_{Rotational Pull-in} = \sqrt{\frac{S_0}{\kappa}} \quad (7)$$

which has been shown in figure (9). It can be seen that even the maximum of the curve at full electrode length is less than the minimum in figure (8). So the rotational pull-in will occur far before vertical pull-in and limits the DC bias that can be applied. It also decreases as we decrease the electrode length hence as shown in figure (7) the sensitivity will not change significantly. This also holds for the change in resonance frequency since the bias range is limited.

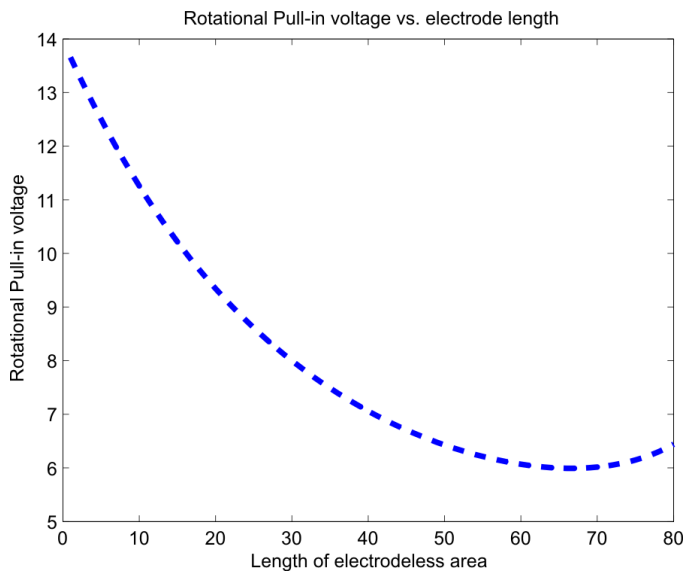


Figure 9. Pull-in voltage results from rotational instability as a function of electrodeless area

III. CONCLUSION

We showed that the sensitivity of biomimetic flow sensor arrays can be optimized by sensibly reduction of the electrode area. This will result in an increase of the electrostatic spring softening (ESS) coefficient as well but also decrease the rotational instability voltage. Therefore applying a DC bias to adapt sensors for a desirable working range will be limited. The maximum sensitivity which can be reached using this

scheme can be changed more by applying DC bias.

ACKNOWLEDGMENT

We like to express sincere gratitude to Meint de Boer and Erwin Berenschot for their advice on processing, Dominique Bouwes (Altpeter) for SU-8 processing, Marcel Dijkstra for generating SEM pictures and our colleagues in the EU project CILIA for stimulating discussions and input to this work.

REFERENCES

- [1] T. Shimozawa, J. Murakami, T. Kumagai, "Cricket wind receptors: thermal noise for the highest sensitivity known", Chapter 10 in *Sensors and Sensing in Biology and Engineering*, ed. Barth, Hamphry and coombs, Springer, Vienna, 2003, ISBN 3-211-83771-X.
- [2] T. Shimozawa et al., "Structural scaling and functional design of the cercal wind-receptor hairs of cricket", *J. Comp. Physiol. A*, 183 (1998), 171-186.
- [3] H. E. de Bree, P. Leussink, T. Korthorst, H. Jansen, T. Lammerink, and M. Elwenspoek, "The Microflown, A Novel Device Measuring Acoustical Flows", *Sensors and Actuators A: Physical*, Volume 54, Number 1, June 1996, pp. 552-557(6).
- [4] J. Chen et al., "Artificial lateral line and hydrodynamic object tracking", *MEMS 2006*.
- [5] Z. Fan et al., "Design and fabrication of artificial lateral line flow sensors", *J. Micromech. Microeng.*, 12 (2002) 655-661.
- [6] Y. Yang et al., "From artificial hair cell sensor to artificial lateral line system: development and application", *MEMS 2007*.
- [7] M. Dijkstra et al., "Artificial sensory hairs based on the flow sensitive receptor hairs of crickets", *J. Micromech. and Microeng.*, 15 (2005), 132-138.
- [8] N. Izadi, R. K. Jaganatharaja, J. Floris and G. Krijnen, "Optimization of Cricket-Inspired, Biomimetic Artificial Hair Sensors for Flow Sensing", *DTIP 2007*.
- [9] S. Chowdhury, M. Ahmadi, and W. C. Miller, "A closed-form model for the pull-in voltage of electrostatically actuated cantilever beams", *J. Micromech. Microeng.* 15 (2005) 756-763.
- [10] G. J. M. Krijnen, J. Floris, M. A. Dijkstra, T. S. J. Lammerink, and R. J. Wiegerink, "Biomimetic micromechanical adaptive flow-sensor arrays", *Proceedings of SPIE Europe Microtechnologies for the New Millennium 2007*, 2-4 May 2007, Maspalomas, Gran Canaria, Spain.